Research article

JGS
Journal of the Geological Society

Published online March 7, 2017

https://doi.org/10.1144/jgs2016-129 | Vol. 174 | 2017 | pp. 655–666

Subsurface biodegradation of crude oil in a fractured basement reservoir, Shropshire, UK

John Parnell*, Mas'ud Baba, Stephen Bowden & David Muirhead

School of Geosciences, University of Aberdeen, Aberdeen AB24 3UE, UK

M.B., 0000-0002-6713-3006

* Correspondence: j.parnell@abdn.ac.uk

Abstract: Subsurface biodegradation of crude oil in current oil reservoirs is well established, but there are few examples of ancient subsurface degradation. Biomarker compositions of viscous and solid oil residues ('bitumen') in fractured Precambrian and other basement rocks below the Carboniferous cover in Shropshire, UK, show that they are variably biodegraded. High levels of 25-norhopanes imply that degradation occurred in the subsurface. Lower levels of 25-norhopanes occur in active seepages. Liquid oil trapped in fluid inclusions in mineral veins in the fractured basement confirms that the oil was emplaced fresh before subsurface degradation. A Triassic age for the veins implies a 200 myr history of hydrocarbon migration in the basement rocks. The data record microbial biodegradation of hydrocarbons in a fractured basement reservoir, and add to evidence in modern basement aquifers for microbial activity in deep fracture systems. Buried basement highs may be especially favourable to colonization, through channelling fluid flow to shallow depths and relatively low temperatures, and are therefore an important habitat within the deep biosphere.

Received 29 September 2016; **revised** 10 January 2017; **accepted** 19 January 2017

Biodegradation is widespread in subsurface oil reservoirs, where the oil provides a ready source of food for microbial activity. Microbial activity is temperature controlled, such that biodegradation is effectively limited by an upper limit of about 80°C, and hence is often depth controlled (Wilhelms *et al.* 2001). Heavy oil, in which lighter components have been preferentially depleted by biodegradation, represents a huge potential resource (Chopra *et al.* 2010). Increasing interest in so-called unconventional reservoirs includes a focus on the potential of fractured basement reservoirs, many of which contain heavy oil, such as in North Africa and the Atlantic Margin (Trice 2014). These buried basement blocks (Fig. 1) are typically durable rocks that have been topographic highs when exposed at the surface before burial, and in some countries are named 'buried hill reservoirs' (e.g. Tong *et al.* 2012). The same properties that make them prominent highs also make them susceptible to brittle deformation, involving fracturing to allow ingress of fluids including hydrocarbons.

We hypothesize that subsurface fractured basement reservoirs are a favourable habitat for microbial activity. Characteristics that would enhance this possibility are as follows: (1) the basement is typically uplifted to a depth (<2 km) at which microbes can thrive; (2) the basement is typically fractured, engendering higher permeability than in matrix porosity; (3) oil-bearing basement provides a food source for microbes; (4) a basement high is typically a focus for structural reactivation, and accompanying fluid movement and replenishment of nutrients; (5) some basement highs reach the surface or near-surface before reburial, when they may be inoculated by microbial assemblages.

Oil and gas are found in basement rocks worldwide, and are exploited in several regions and countries, including the USA, North Africa, China and SE Asia (P'An 1982; Petford & McCaffrey 2003; Schutter 2003). The basement habitat is, therefore, potentially very important and merits investigation for evidence of its occurrence. In this study, we examine exhumed fractured Precambrian basement, containing extensive oil residues, in Shropshire, onshore UK, and assess the distribution of microbial activity using organic molecular biomarker evidence for biodegradation. The oil residues are degraded to bitumen (*sensu lato*; very viscous to brittle solid). In this case, as the rocks are exposed at the surface, the degradation could be a recent feature. Oil is actively seeping through aquifers in overlying sandstones, and so is susceptible to surficial alteration. Alternatively, the bitumen could represent an exhumed basement reservoir, in which alteration occurred during a much earlier phase of oil charge and biodegradation. We investigate the origin of the bitumen by (1) assessment of whether the bitumen shows signatures of biodegradation, (2) if it does, assessment of whether biodegradation was a more recent or ancient feature, and (3) constraining the thermal history of the bitumen, its source rock and the host fracture system.

Geological setting

The region of study is in Shropshire, part of the 'Welsh Borderland'. The main components of the hydrocarbon migration story in the region (Fig. 2) are as follows: (1) a block of pre-Carboniferous rocks, including Longmyndian and Uriconian (late Proterozoic) metasediments and metavolcanic rocks, and a succession of Cambrian to Devonian sediments; (2) a Carboniferous coal-bearing succession, in a thick basin to the east (Stafford Basin), and as a thin veneer on the pre-Carboniferous block; (3) a Triassic basin to the north (Cheshire Basin). The Triassic basin is bounded to the east by a major lineament, the Red Rock Fault, which extends southwards as the Hodnet Fault and Church Stretton Fault (Fig. 2), which cut the pre-Carboniferous block. These major NE–SW-trending faults have a long multi-phase history, from Precambrian to Triassic (Woodcock 1984). Subsidiary, cross-cutting faults, trending WNW–ESE to ENE–WSW, also have a multi-phase history, up to the Triassic, and exhibit lateral displacements (Pocock *et al.* 1938; Greig *et al.* 1968). The pre-Carboniferous block is a topographic high, owing to very durable late Proterozoic rocks that were deformed or metamorphosed in the Cadomian Orogeny (Pauley 1990; Compston *et al.* 2002). The block was a positive feature, relative to the Carboniferous sediments, at the time of

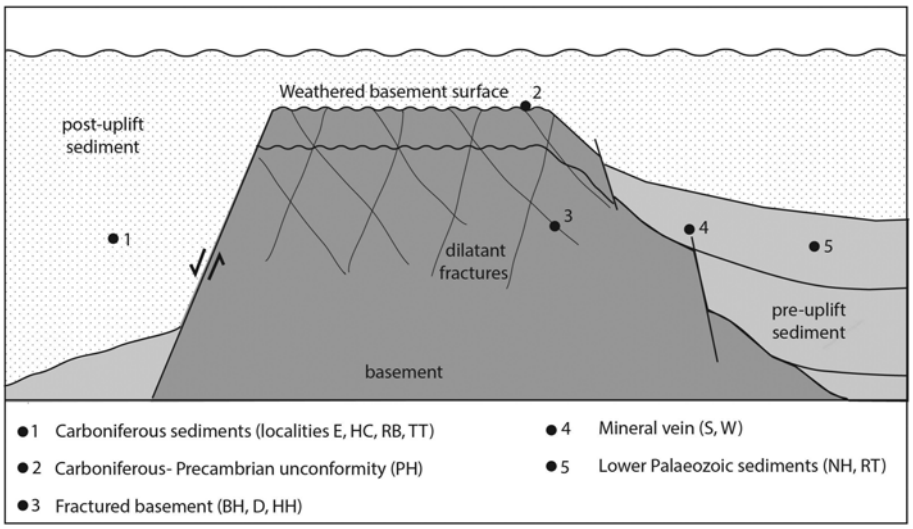

Fig. 1. Schematic section through potential fractured basement reservoir. Settings for samples (key in Fig. 2) are shown for case in Shropshire where basement is Precambrian, pre-uplift sediments are Lower Palaeozoic and post-uplift sediments are Carboniferous.

Triassic deposition, as evidenced by a Triassic–Precambrian unconformity (Pocock *et al.* 1938). Uplift of the block, along with faulting and folding, occurred during the Carboniferous–Permian Variscan Orogeny.

Hydrocarbons (residues of solid bitumen) occur in the Triassic, Carboniferous and the Pre-Carboniferous block, the last including bitumen in fractured Longmyndian metasediments, Cambrian sandstones and mineral veins (Parnell *et al.* 1991). The vein system is related to Triassic basin extension (Plant *et al.* 1999), and is mineralized by barite in Longmyndian metasediments, and galena–sphalerite in Ordovician sediments, where these rocks are cut by the WNW–ESE to ENE–WSW faults. Biomarker evidence indicates an origin for the bitumen in Carboniferous source rocks (Didyk *et al.* 1983; Parnell *et al.* 1991). Thermal maturation of coals and shales in the Carboniferous, to generate hydrocarbons, probably commenced during the late Carboniferous in the Stafford Basin to the east, and during the Triassic in the Cheshire Basin to the north (Plant *et al.* 1999). Hydrocarbon generation could have continued in both basins until Palaeogene uplift. The occurrence of bitumen in the Triassic-aged vein system indicates Triassic or post-Triassic migration, and is consistent with the timing of hydrocarbon generation in either basin.

Methods

Bitumen samples

Bitumens were sampled (Fig. 2; Table 1) in three settings. First, some bitumen occurs flowing as a viscous liquid in aquifers exposed at the land surface. This includes bitumen in Carboniferous sandstones at the Tar Tunnel, Coalbrookdale; bitumen floating on the surface of a water well in Longmyndian metasediments at Pitchford Hall; and bitumen seeping through mine workings at the Wrentnall barite mine and Snailbeach lead–zinc mine. Second, bitumen occurs in fractured Longmyndian metasediments (Fig. 3) in quarry workings at Bayston Hill and Haughmond Hill, and at a surface exposure at Downton. The quarries are exploited for roadstone, as the metasediments are exceptionally durable. In these quarries the bitumen is largely solid but may be a very viscous liquid when freshly exposed by quarrying. Similarly, bitumen in Carboniferous sandstones on the Longmyndian unconformity surface at Row Brook is solid, but was once quarried as an oil sand from which oil was distilled (Plot 1684; Ele 1697). Solid bitumen in Carboniferous sandstone is also exposed on the River Severn at Emstrey. Third, solid bitumen infills the remaining porosity in well-cemented Cambrian sandstones at Robins Tump, and in Ordovician sandstones at Nills Hill. The bitumen pervasively fills microporosity (Parnell 1987), and so must have entered as a low-viscosity oil and solidified in place. Control samples of vein bitumen from the Jurassic Newark Group, Connecticut, USA and the Devonian Orcadian Basin, Orkney, UK (Parnell & Monson 1995; Parnell *et al.* 1998) were analysed to allow comparison with bitumen that had migrated directly from the source rock rather than via near-surface seepages, and so should not exhibit biodegradation. The background thermal maturity was measured from coal samples at Row Brook and Hanwood Colliery (Fig. 2).

Criteria for subsurface biodegradation

The assessment of a subsurface origin for biodegradation is based upon three approaches: petrography, organic geochemistry and thermal history. Petrographic studies can help to assess if bitumen was emplaced as a degraded solid rather than as low-viscosity oil. Organic biomarkers can be used to distinguish biodegradation in the geological record from more recent biodegradation. Biomarkers in coals, and fluid inclusions in mineral veins, can constrain the levels of heating experienced by the rocks from the Carboniferous onwards, and hence whether temperatures were suitable for microbial activity.

The depth at which biodegradation occurred is assessed using altered forms of hopanes and steranes. We particularly use the occurrence of 25-norhopanes as an indicator of subsurface biodegradation. These compounds are observed to be associated with known examples of biodegradation (e.g. Peters *et al.* 1996; Bennett *et al.* 2006; Wang *et al.* 2013; Lamorde *et al.* 2015), but only in samples from subsurface settings. They are not recorded from surface heavy oil seepages. The formation of 25-norhopanes through the microbial removal of the methyl group at C-10 within the hopane nucleus during the biodegradation of petroleum is widely reported (Bennett *et al.* 2006, and references therein). Concentrations of 25-norhopanes increase downwards, towards the oil–water contact (Bennett *et al.* 2006; Wang *et al.* 2013), and correlate with the degree of biodegradation (Bennett *et al.* 2006; Lamorde *et al.* 2015). This suggests that their formation requires anaerobic conditions and typically under burial >100 m. They have been recorded in oils back to at least the Silurian (Wang *et al.* 2015). Degradation is also reflected in the ratio of diasteranes to steranes. Diasteranes are formed by a rearrangement of steranes during diagenesis and thermal maturation. Biodegradation causes the breakdown of steranes at a faster rate than diasteranes hence the diasterane/sterane ratio can be exploited as a measure of shallow biodegradation (Seifert & Moldowan 1979).

Table 1. *Biomarker data for samples of bitumen*

Locality	Grid reference	Host age	Host lithology	Setting	Height a.s.l. (m)	Sterane (μg g^{-1})	Diasterane (μg g^{-1})	Sterane/ diasterane	C30-hopane	C29-norhopanes	C29-norhopane/ C30-hopane	25-norhopanes (μg g^{-1})	Regular hopanes (μg g^{-1})	Norhopanes/ regular hopanes	C29 20S/(20S + 20R)
Tar Tunnel	SJ694026	Carboniferous	Sandstone	Seepage in pools	40	0.62	0.18	3.44	22.28	3.60	0.14	22.66	77.52	0.31	0.43
Row Brook 1	SJ532046	Carboniferous	Basal breccia	Pore-filling	70	0.78	0.25	3.12	27.22	5.47	0.17	33.45	87.34	0.40	0.52
Row Brook 2	SJ532046	Carboniferous	Basal breccia	Pore-filling	70	0.04	0.02	2	0.63	0.16	0.20	0.94	1.74	0.56	0.51
Emstrey	SJ518112	Carboniferous	Sandstone	Pore-filling	50	0.06	0.03	1.72	0.23	0.59	1.97	3.94	5.83	0.68	0.60
Pitchford Hall (2015)	SJ528043	Proterozoic	Metasediment	Water well	80	1.89	0.48	3.94	46.38	9.22	0.17	38.57	66.23	0.39	0.45
Pitchford Hall (2009)	SJ528043	Proterozoic	Metasediment	Water well	80	1.67	0.74	2.26	22.62	6.80	0.23	52.77	142.03	0.58	0.53
Bayston Hill	SJ495095	Proterozoic	Metasediment	Fracture-filling, with quartz	80	0.05	0.02	2.86	1.34	0.14	0.10	1.10	3.47	0.32	0.56
		Proterozoic	Metasediment	With calcite		0.03	0.02	1.2	4.29	2.85	0.16	6.02	16.07	0.40	1.00
		Proterozoic	Metasediment	With calcite		0.001	0.001	1.52	0.07	0.06	0.19	0.11	0.21	0.52	0.44
		Proterozoic	Metasediment	Pure bitumen		0.04	0.03	1.22	1.63	0.41	0.20	2.63	3.94	0.67	0.59
Haughmond Hill	SJ542145	Proterozoic	Metasediment	Fracture-filling, with barite	100	4.07	1.25	3.25	52.68	66.10	0.32	321.58	163.51	0.54	0.39
		Proterozoic	Metasediment	With calcite		0.02	0.01	1.31	1.69	0.55	0.25	3.57	4.47	0.80	0.33
		Proterozoic	Metasediment	With chlorite		0.64	0.17	3.77	17.13	5.35	0.24	34.28	55.01	0.62	0.54
		Proterozoic	Metasediment	Pure bitumen		2.16	0.89	2.42	90.70	15.93	0.15	282.66	101.47	0.38	0.49
Downton	SJ542130	Proterozoic	Metasediment	Fracture-filling	100	0.015	0.004	3.87	0.26	0.08	0.22	0.40	0.66	0.61	0.47
Wrentnall 1	SJ418032	Proterozoic	Metasediment	Barite vein	210	0.07	0.05	1.54	2.21	0.76	0.25	4.97	7.20	0.69	0.32
Wrentnall 2	SJ418032	Proterozoic	Metasediment	Barite vein	210	0.01	0.002	3.98	0.28	0.09	0.24	0.50	0.96	0.53	0.45
Snailbeach	SJ377022	Ordovician	Sandstone	Pb–Zn vein	250	0.71	0.25	2.83	16.16	3.53	0.18	21.63	48.63	0.47	0.47
Nills Hill	SJ295032	Ordovician	Sandstone	Pore-filling	150	0.05	0.02	2.26	0.91	0.22	0.19	1.42	2.13	0.67	0.68
Robin's Tump 1	SO483954	Cambrian	Sandstone	Pore-filling	290	0.10	0.03	3.95	0.35	nd	nd	nd	5.20	nd	0.56
Robin's Tump 2	SO483954	Cambrian	Sandstone	Pore-filling	290	0.05	0.03	1.99	0.30	nd	nd	nd	2.88	nd	0.62
Orkney		Devonian control	Mudrocks	Fracture-filling		0.01	0.004	1.78	0.34	nd	nd	nd	0.40	nd	0.66
Connecticut		Jurassic control	Mudrocks	Fracture-filling		0.02	0.74	0.02	0.26	nd	nd	nd	0.26	nd	0.48

nd, not determined.

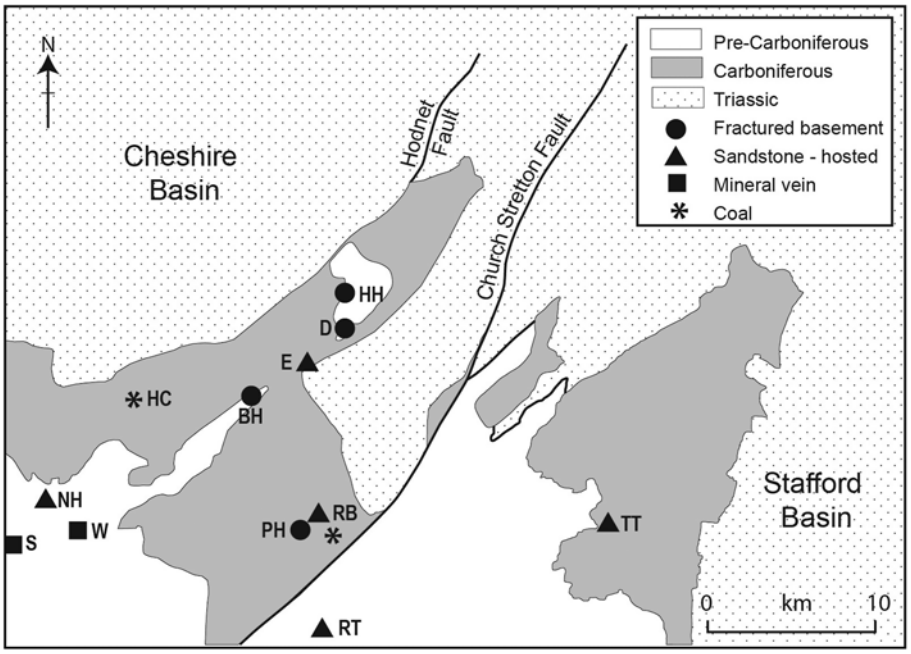

Fig. 2. Outline geological map of region of Shropshire including sample sites. BH, Bayston Hill; D, Downton; E, Emstrey; HC, Hanwood Colliery; HH, Haughmond Hill; NH, Nills Hill, PH, Pitchford Hall, RB, Row Brook; RT, Robin's Tump; S, Snailbeach; TT, Tar Tunnel; W, Wrentnall.

Biomarkers

Rock samples were prepared by rinsing with distilled water two times, and again with dichloromethane (DCM). The dry rocks were crushed and extracted using a Soxhlet apparatus for 48 h. Solid bitumen and tar samples were ultrasonicated with DCM and methanol (MeOH). All glassware was thoroughly cleaned with a 93:7 mixture of DCM–MeOH. Crushed samples were weighed, recorded and transferred into pre-extracted thimbles. The extracts were then dried down using a rotary evaporator, separated into aliphatic, aromatic and polar fractions via a silica column chromatography using hexane, hexane–DCM in the ratio 3:1 and DCM–MeOH respectively. Prior to gas chromatography–mass spectrometry (GC–MS) analysis, an internal standard (5β-cholane, Agilent Technologies) was added to the aliphatic fraction before injection into the GC–MS machine and subsequent biomarker identification. This was done using an Agilent 6890N gas chromatograph fitted with a J&W DB-5 phase 50 m mass selective detector and a quadruple mass spectrometer operating in selected ion monitoring mode (dwell time 0.1 s per ion and ionization energy 70 eV). Samples were injected manually using a split/splitless injector operating in splitless mode (purge 40 ml min^{-1} for 2 min). The temperature programme for the GC oven was 80 – 295°C, holding at 80°C for 2 min, rising at 10°C min^{-1} for 8 min and then 3°C min^{-1}, and finally holding the maximum temperature for 10 min. Quantitative biomarker data were obtained for isoprenoids, hopanes, 25-norhopanes, steranes and diasteranes by measuring responses of these compounds on *m*/*z* 85, 191, 177, 217, 218 and

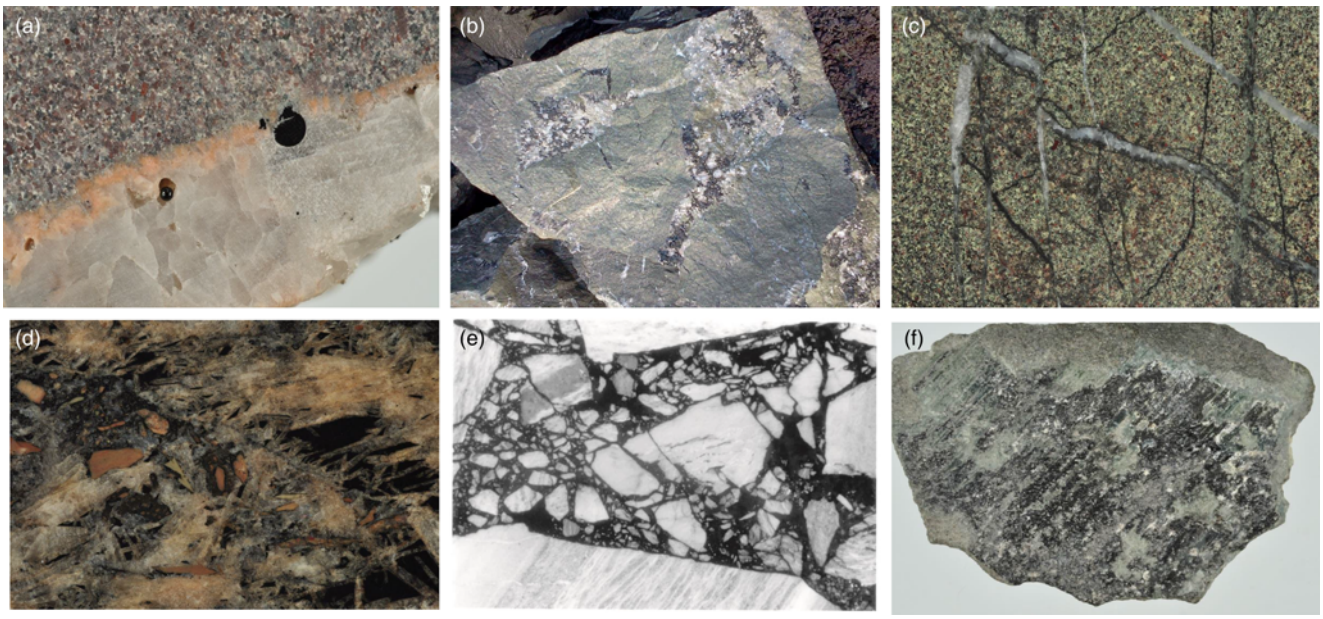

Fig. 3. Bitumen in Longmyndian metasediments, in hand specimen. (**a**) Bitumen in globules in quartz-lined fractures, Bayston Hill; (**b**) fracture surface coated with mixed calcite and bitumen, Bayston Hill; (**c**) close-up of mineralized fractures, showing multiple generations of both calcite and bitumen, Bayston Hill; (**d**) fracture-fill barite crystals mixed with bitumen, cut by breccia zone containing wallrock fragments, Haughmond Hill; (**e**) breccia zone of wallrock fragments suspended in bitumen, Downton; (**f**) bitumen-coated fracture, subsequently slickensided, Haughmond Hill. Field widths: (**a**) 5 cm; (**b**) 25 cm; (**c**) 2 cm; (**d**) 6 cm; (**e**) 5 cm; (**f**) 10 cm.

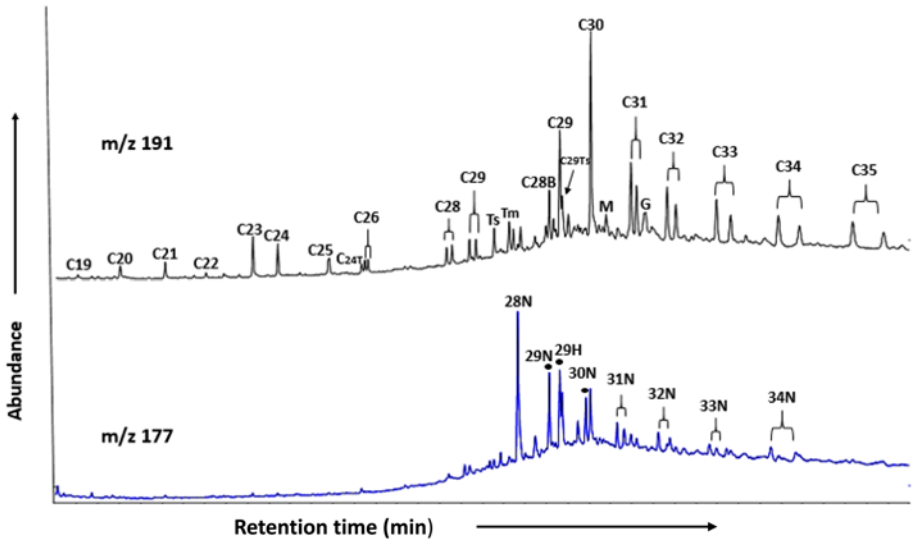

Fig. 4. Ion chromatograms for *m/z* 191 and 177, showing identification of hopanes and norhopanes.

259 mass chromatograms and comparing them with the response of the internal standard. Thermal maturity was estimated from the 20S/(20S + 20R) ratio for C_{29} steranes, based on the increasing proportion of the S isomer with maturation (Peters & Moldowan 1993).

Selected samples of bituminous rocks from Haughmond Hill and Bayston Hill quarries were examined using an ISIS ABT-55 scanning electron microscope with Link Analytical 10/55S EDAX facility.

Fluid inclusions

Fluid inclusion studies were performed on doubly polished wafers using a Linkam THMS-600 heating–freezing stage mounted on a Nikon Labophot transmission light microscope. The instrument, equipped with a range of objective lenses including a 100× lens, was calibrated against synthetic H_2O (374.1 and 0.0°C) and CO_2 (−56.6°C) standards (Synthetic Fluid Inclusion Reference Set, Bubbles Inc., USA). The petrography of fluid inclusion assemblages was first examined at low magnifications using a NIKON Eclipse E600 microscope equipped with both transmitted white and incident ultraviolet light (UV) sources. Ultraviolet light, with an excitation wavelength of 365 nm, was provided by a high-pressure mercury lamp with a 420 nm barrier epi-fluorescence filter that allows only the long-wavelength UV to reach the sample.

Results

Biomarker data

The sample set as a whole shows a spread of compositions in terms of the indicators of biodegradation (Figs 4 – 6; Table 1). Some samples provide evidence of conversion of hopanes to norhopanes (peak identification shown in Fig. 4) and could be considered to have been biodegraded to a biodegradation level of 9 on the scale of Peters & Moldowan (1993). However, not all samples demonstrate sterane alteration. Therefore, although all samples are very heavily biodegraded, the patterns of biomarker alteration are variable. Thus three broad fields can be distinguished (Fig. 6). As expected, those samples that show least evidence of biodegradation (lowest ratios of diasterane/sterane, norhopane/hopane) are those that are least viscous and were collected from active seepages. These are the samples from the Tar Tunnel, the well at Pitchford Hall, and bitumen from a recent seepage at Bayston Hill. The more degraded samples are immobile solids. The most degraded samples are mineralized samples from both quarries and the Wrentnall mine, and also the Carboniferous sandstone at Emstrey. The calcite-bearing samples have relatively low sterane/diasterane ratios. This could reflect an origin for the carbonate in the microbial oxidation of oil under near-surface conditions, which would be associated with the biodegradation of steranes. The two samples from Robin's Tump yielded no 25-norhopanes. The control samples of vein bitumen from other sequences also have no 25-norhopanes.

Bitumen-bearing fractures

The bitumen-bearing fractures at Bayston Hill and Haughmond Hill are in sandstones and conglomerates, which exhibit extensive brittle fractures in multiple orientations, especially trending WNE–ESE to ENE–WSW. Most of the fractures are subvertical to vertical. The bitumen-bearing fractures include the following.

(1) Fractures (tight, up to 1 mm width aperture) containing only bitumen, which may be cut by later fractures containing calcite–bitumen mixtures.
(2) Fractures (tight, up to 3 mm width aperture), lined with authigenic quartz (Fig. 3) and/or albite overgrowing detrital quartz in the host sandstone, coated with bitumen, then cut by later fractures containing calcite–bitumen mixtures. The quartz contains inclusions of bitumen (see below).
(3) Fractures (large open, up to ≥5 cm width aperture) mineralized by bladed barite (Fig. 3), with remaining porosity infilled by bitumen, then cut by later fractures containing calcite–bitumen mixtures.
(4) Fractures containing variable mixtures of calcite, bitumen and less commonly chlorite. Cross-cutting relationships suggest multiple episodes of calcite–bitumen veining (Fig. 3). Bitumen–calcite mixtures also contain clasts of country rock in breccia zones, and some bitumen-bearing fractures show brecciation associated with bitumen emplacement.

In addition, traces of sulphides (pyrite, copper sulphides) occur in the quartz, bitumen and calcite.

Authigenic mineralogy

Petrographic studies of the host sandstones from the two quarry sites show a markedly different mineral assemblage in samples that contain bitumen. All samples contain an authigenic mineral assemblage of quartz, illitic clay, chlorite, iron–titanium oxides and epidote that is unrelated to, and cross-cut by (and so predates),

the bitumen. The bitumen-bearing samples contain additional minerals, which form coatings to vugs and fractures that are otherwise filled with bitumen. The earliest pore-coating is consistently albite, which is overgrown by potassium feldspar (Fig. 7). Additional phases include authigenic apatite, titanite and crystals of titanium oxide with a bladed morphology characteristic of brookite (Fig. 7). Authigenic quartz occurs both as a pore-coating and as euhedra suspended within bitumen (Fig. 7). The bitumen appears to have co-deposited with this mineral assemblage, as evidenced from complex intergrowths between bitumen and feldspar–quartz (Fig. 7), and crystals of brookite and quartz suspended within bitumen. This assemblage predated calcite-bearing fractures.

Pyrite and copper sulphides occur in three settings, as follows.

(1) Sulphides are associated with the primary vein mineralization at Snailbeach and Wrentnall. The veins provide porosity for later oil or bitumen ingress, so these sulphides are unrelated to oil degradation.

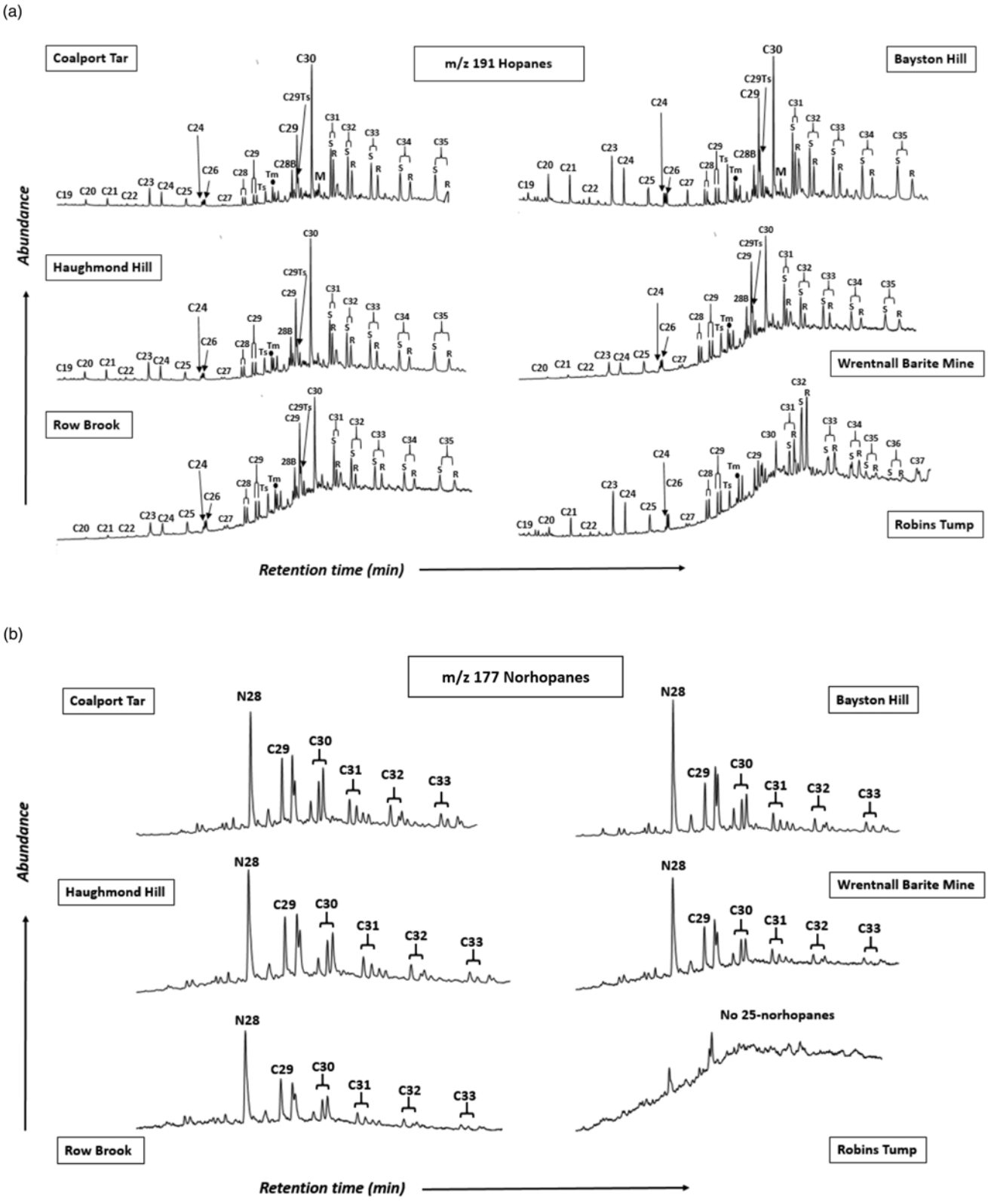

Fig. 5. Selected ion chromatograms for (**a**) *m*/*z* 191, highlighting normal hopanes, (**b**) *m*/*z* 177 for norhopanes.

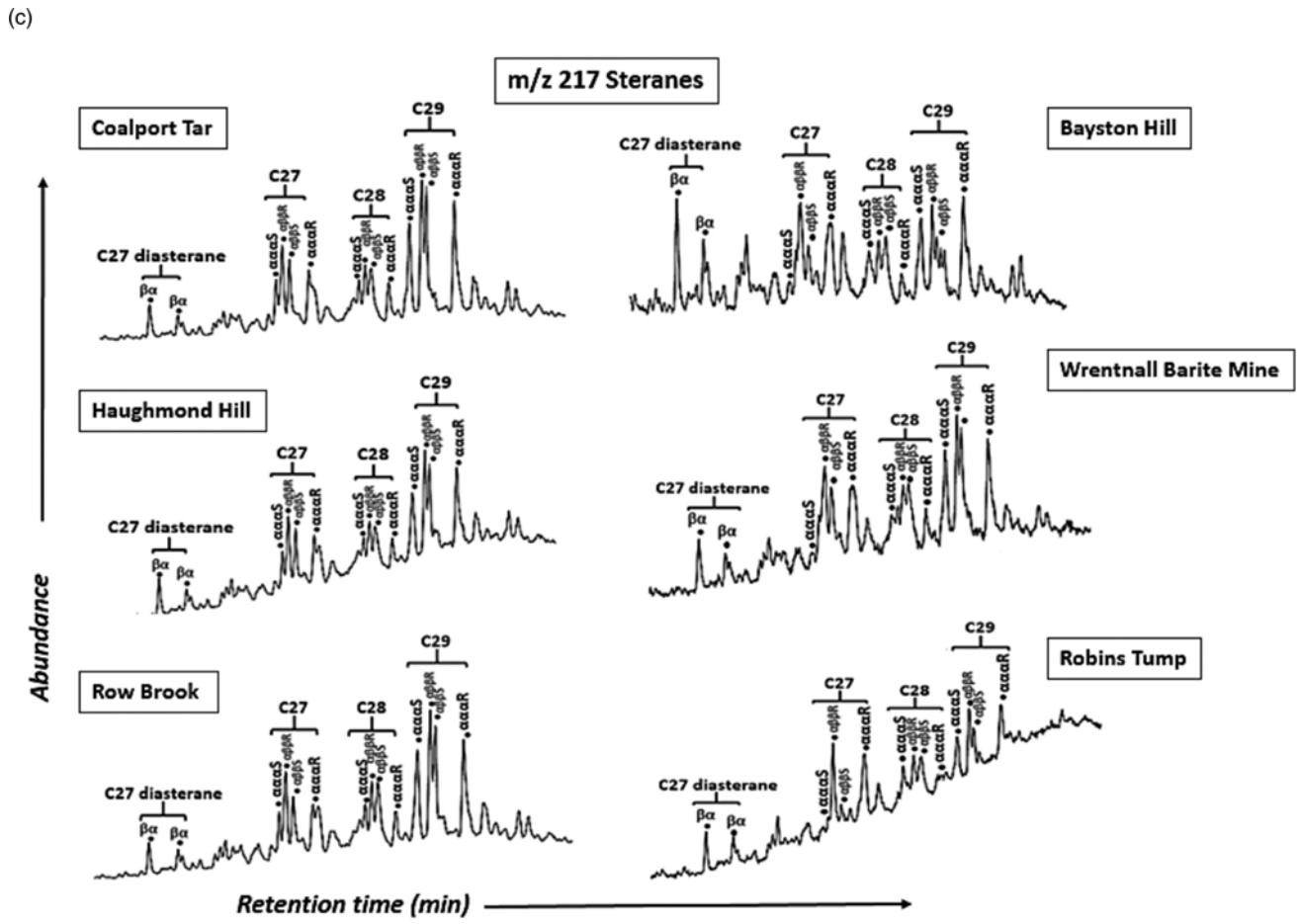

Fig. 5. *Continued*. (**c**) *m*/*z* 217 for steranes.

(2) Pyrite occurs in the quartz and calcite that are coeval with some bitumen in veins, and also occurs in the bitumen itself. Sulphides are most abundant in sandstone that contains bitumen-bearing fractures, and are located particularly within or at the margin of the bitumen (Fig. 7d). This was observed especially in the quartz- or calcite-bearing samples analysed from Haughmond Hill.

(3) The bitumen at Row Brook is post-dated by framboidal pyrite (Bata & Parnell 2014).

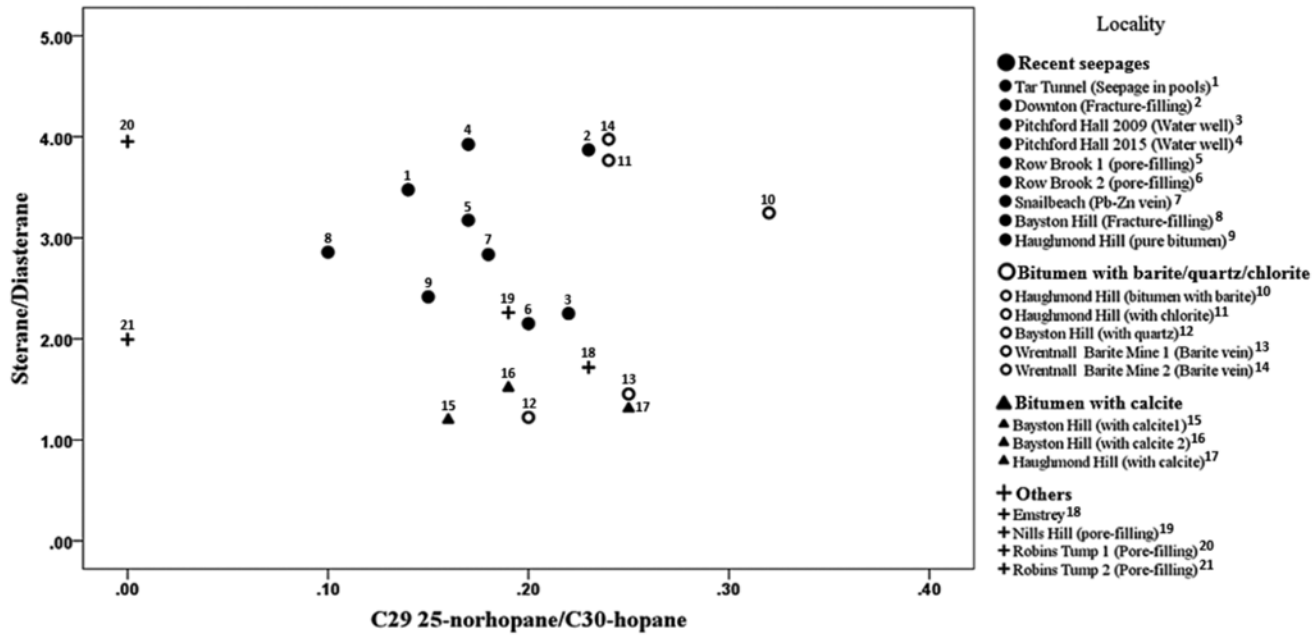

Fig. 6. Cross-plot of sterane and hopane maturity parameters. Recent seepages show lower norhopane/hopane ratios then mineralized samples.

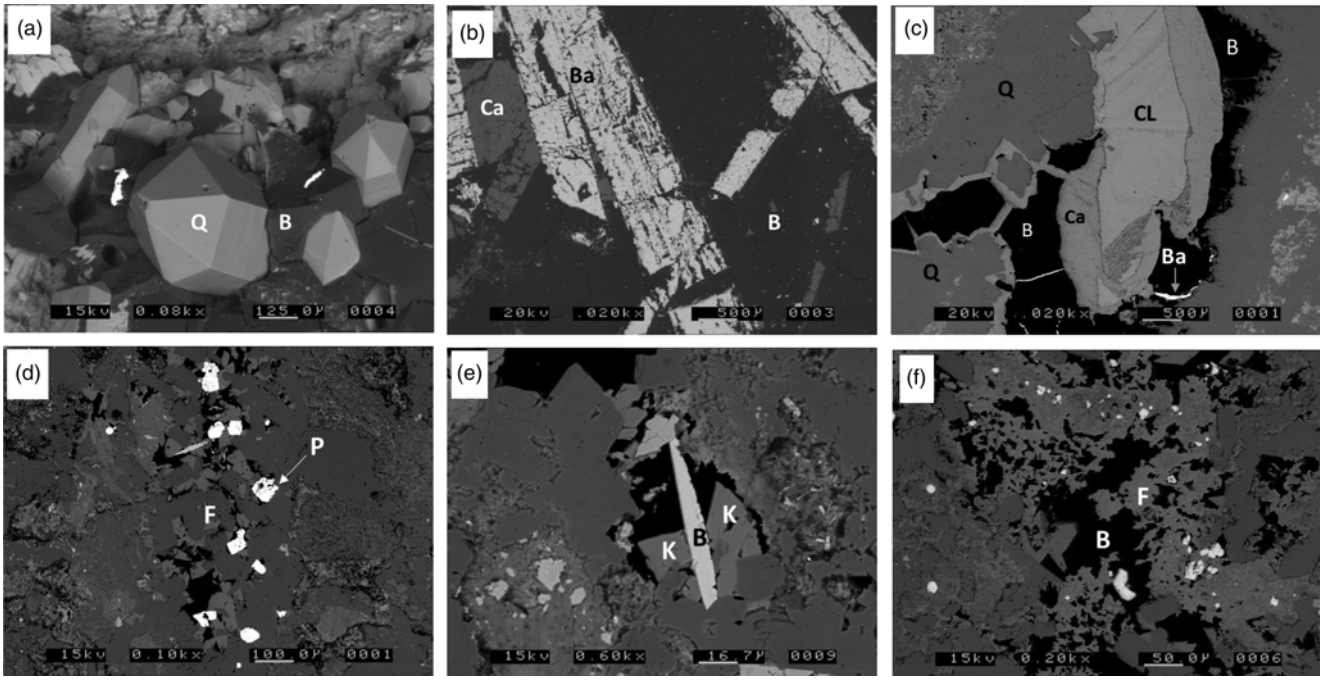

Fig. 7. Scanning electron photomicrographs of bitumen in Longmyndian metasediments. (**a**) Authigenic quartz (Q) in bitumen (B); (**b**) barite (Ba) and calcite (Ca) crystals in bitumen (B); (**c**) chlorite (CL), calcite (Ca), quartz (Q) and barite (Ba) in bitumen (B); (**d**) pyrite crystals (bright) in bitumen (dark) and mixed potassium feldspar and albite (F); (**e**) brookite (B) and potassium feldspar (K) in bitumen (dark); (**f**) intermixed feldspars (F) and bitumen (B). (**a**) Bayston Hill; (**b**–**f**) Haughmond Hill.

Paragenetic sequence

The combination of evidence from fractures and sandstone petrography allows the reconstruction of a paragenetic sequence established from cross-cutting relationships evident in hand specimen and electron microscopy (Fig. 8). The occurrence of oil fluid inclusions in some mineral phases helps to incorporate hydrocarbons into the paragenesis. Hydrocarbons are present in the early quartz and feldspar pore or fracture coatings, as entrapped bitumen globules (Fig. 3) and oil fluid inclusions in quartz, and also in the later calcite veins, as overlapping calcite–bitumen mixtures (Fig. 3) and oil fluid inclusions in calcite.

Although some bitumen appears to be filling residual porosity, there is also evidence that in some veins the bitumen migrated forcefully. Hairline veinlets of bitumen are filled to their tips, which is characteristic of a fracture formed by the infilling fluid; and the

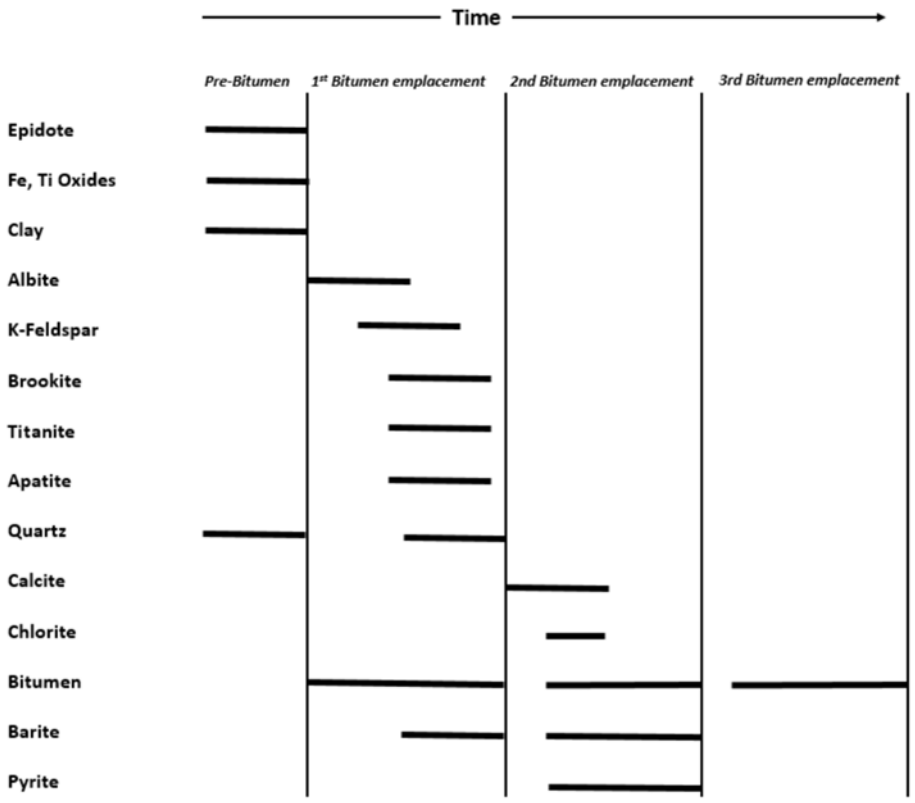

Fig. 8. Paragenesis of bitumen-bearing fractures, based on petrographic study of samples from Bayston Hill and Haughmond Hill quarries.

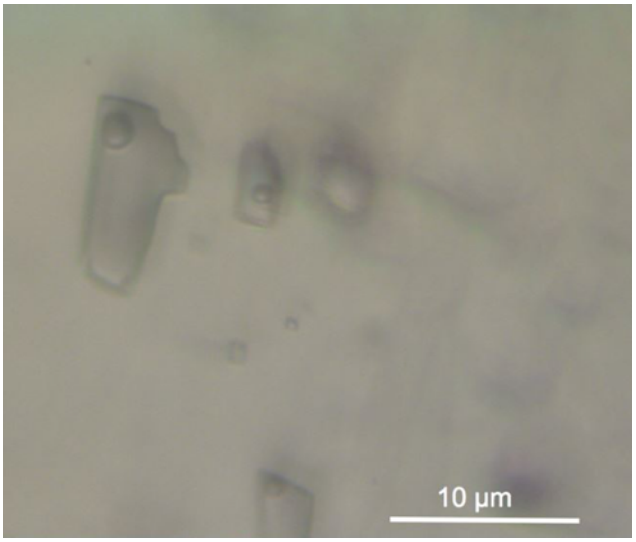

Fig. 9. Photomicrograph of two-phase fluid inclusions in calcite, Bayston Hill. Inclusions fluoresce bluish white under UV light.

evidence of brecciation during bitumen emplacement suggests a vigorous migration. Some bitumen surfaces exhibit slickensides (Fig. 3), indicating fault movement since bitumen emplacement.

Thermal history

Thermal history is constrained by the maturity of organic matter and by fluid inclusion data from minerals.

The maximum temperature experienced by the rocks hosting the bitumen is indicated by temperature-sensitive biomarkers in Carboniferous rocks lying unconformably on the pre-Carboniferous blocks, especially coals. Sterane C_{29} $\alpha\alpha$ 20S/(20S + 20R) values from the two coal deposits of 0.36 (Row Brook) and 0.37 (Hanwood Colliery) indicate mid oil window maturities; that is, temperatures up to 100°C.

The bitumen is assumed to be derived from oil expelled from adjacent sedimentary basins, where Carboniferous source rocks experienced greater burial depths than on the blocks. Sterane C_{29} $\alpha\alpha$ 20S/(20S + 20R) values mostly in the range 0.4 – 0.5 from the bitumens indicate mid to late oil window maturity.

Fluid inclusion data are available from vein minerals calcite, quartz and barite, cutting the pre-Carboniferous blocks. Both oil and aqueous primary fluid inclusions (Fig. 9) occur in each mineral. The

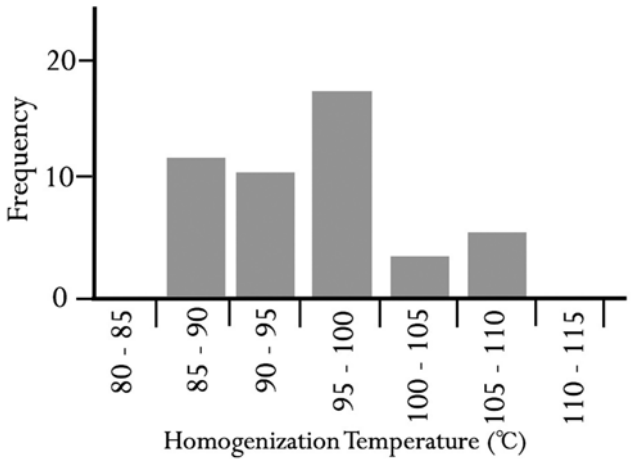

Fig. 10. Homogenization temperatures for calcite-hosted fluid inclusions, Bayston Hill.

oil and aqueous inclusions appear to be coeval, but no mixed fluid infills were observed. Inclusions in calcite and quartz–barite are up to 24 µm and 5 µm size respectively. The largest inclusions in the calcite are isolated or in small clusters, whereas smaller inclusions occur abundantly in planes parallel to crystal growth surfaces. Homogenization temperatures for aqueous inclusions in the calcite are in the range 85 – 125°C (Fig. 10). Inclusions in the quartz and barite are too small for microthermometry, but the largest examples are two-phase and liquid-rich (Fig. 9); these features are typical of temperatures comparable with those recorded from the calcite-controlled inclusions. The blue–white fluorescence of the oil fluid inclusions is typical of liquid oil generated at peak oil generation (e.g. Bodnar 1990; Parnell *et al.* 2001).

Discussion

Fracturing of the basement

It is evident that the pre-Carboniferous block has been uplifted at several times, including during the Carboniferous (only the latest Carboniferous is present in the cover sequence), post-Carboniferous (evidenced by local Triassic–Proterozoic unconformity) and post-Triassic (currently elevated above the Triassic basin). Multiple episodes of uplift provide multiple opportunities for fluid ingress. Uplift creates a geometry that focuses fluid flow (Fig. 1), including hydrocarbons and mineralizing fluids, towards the basement.

It is no coincidence that the rocks containing the bitumen-bearing fractures are currently being exploited for roadstone. They are extremely durable (they have a high Polished Stone Value rating), and Bayston Hill rock has accordingly been used in the M6 toll motorway. This characteristic has made them susceptible to deformation by brittle fracturing. They have probably experienced multiple episodes of fracturing, including the uplift events noted above, but regional Triassic extension would have been a particularly likely time for dilatant fracture formation and is considered responsible for the barite and lead–zinc mineralization (Plant *et al.* 1999).

Migration into the fractured basement

Within the area of study (Fig. 2), the pre-Carboniferous block was formerly covered by Carboniferous sediments, which survive as coal-bearing sequences at the margins of the block. At many sites, the depth of penetration of bitumen below the sub-Carboniferous unconformity into the basement is difficult to assess. However, at the two quarry sites, minimum depths of 60 m (Bayston Hill) and 93 m (Haughmond Hill) can be attributed, based on the exposed sections of Proterozoic metasediments below the current land surface. Allowing for limited erosion of the pre-Carboniferous block, a minimum depth of 100 m penetration of bitumen is deduced. This estimate is based on penetration vertically downwards, which is consistent with vertical to subvertical fracture systems observed in the quarries. However, as both sites are topographically above Carboniferous rocks, migration pathways were probably lateral and much longer than those for vertical migration. At the Pitchford Hall locality, which is a water well at the Carboniferous–Proterozoic unconformity, bitumen floats on the water surface, and so must have separated from the water below. Historical records confirm that bitumen recharges into the well from below (e.g. Camden 1722), indicating a migration pathway in the Proterozoic rocks that is not downward directed. Most of the samples in the pre-Carboniferous rocks are from close to the projected sub-Carboniferous unconformity, where oil could readily penetrate into porous zones below the unconformity. In the west of the region, the bitumen-bearing mineral vein system in the pre-Carboniferous block, at Wrentnall, Snailbeach and other localities,

extends laterally to the Proterozoic–Carboniferous unconformity (Dines 1958; Pattrick & Bowell 1991). The barite mine at Wrentnall was 1 km west from a coal mine, and at a topographically higher level, thus lateral migration from Carboniferous to Proterozoic is very possible. Like Wrentnall, most of the sub-Carboniferous bitumen-bearing localities are above the Carboniferous sites (Table 1), as is typical for 'buried hill' geometry (Fig. 1).

Paragenesis

The paragenesis for the quarry sites (Fig. 8) can be divided into four phases: a pre-fracturing phase when the rock became tightly cemented and epidotized by mild metamorphism; a fracturing phase dominated by quartz–feldspars–barite–bitumen; a fracturing phase dominated by calcite–chlorite–bitumen; post-mineralization fracturing in which viscous bitumen still seeps today.

The Triassic age of the barite mineralization (Plant *et al.* 1999) and the continued seepage today imply that migration has occurred over at least 200 myr. Evidence of deformation (breccia zones, slickensides) is associated with the third (calcite, chlorite) stage of paragenesis, but cannot be specifically dated. The first three stages involve mineralization, and clearly date to deep geological time, whereas the final stage may be related to modern or recent seepage.

The authigenic mineralogy associated with the second paragenetic phase is unusual, in containing titanite and brookite, but both are recorded as sandstone cements elsewhere (Morad 1986; van Panhuys-Sigler & Trewin 1990). The co-deposition of bitumen with authigenic feldspars and quartz is, notably, also observed in another example of hydrocarbons in fractured Precambrian basement, in the Moinian of Scotland (Parnell 1996). Possibly the ingress of fluid from above, into freshly fractured metamorphic rock with which it is not in geochemical equilibrium, allowed ready dissolution of mineral surfaces and reprecipitation of the unusual mineral assemblage.

Palaeotemperature

The maturation levels reported here for the coals confirm that the Carboniferous succession in the immediate vicinity of the bitumen occurrences had entered the oil window and so would have generated hydrocarbons. These coals must have been buried to at least 2 km to reach the oil window. Higher maturities recorded in the bitumens suggest a source from a deeper (thicker) Carboniferous succession. Evidence from the Carboniferous succession preserved in the adjacent Stafford Basin (Hamblin & Coppack 1995) suggests that this burial could have been achieved during the Carboniferous. Once the oil had flowed to the shallower (topographically higher) sites in the pre-Carboniferous basement, it would have been cooler than in the source kitchen. This contrast between the cooler uplifted basement and the warmer surrounding sedimentary basin is a characteristic of the 'buried hill' geometry (Fig. 1).

The mineral vein fluid inclusion temperatures in the range 85–125°C represent rapidly expelled deep basin fluids, hotter than the ambient host rock, which probably did not exceed 100°C. These relatively hot temperatures must have been short-lived, as the fluids would have equilibrated with the cooler host rock, and so may not have influenced the organic maturation, measured in the coal samples and experienced by the rocks generally. They are also not so hot that they would have caused the breakdown of oil to gas. The contrast between high temperatures in ephemeral fluids and low temperatures in the host rock is a common feature of subsiding basins (Parnell 2010). It is, therefore, reasonable to envisage oil being introduced through the fracture systems without being destroyed by the thermal conditions. It should be noted that the occurrence of chlorite does not signify high temperatures, as chlorite in reservoir rocks may form during near-surface diagenesis (Grigsby 2001). Once the temperature had equilibrated with that of the host rock, the oil temperature would have been low enough to support microbial activity, especially where oil had flowed from the Carboniferous into subjacent rocks.

Biodegradation

Almost all samples yield 25-norhopanes, which is consistent with all having a history of biodegradation in the subsurface. 25-norhopanes are found in samples from each of the three fracturing stages (Fig. 8) in the paragenetic history. However, the samples showing most evidence of degradation are those from mineralized fractures. The earliest stage quartz–barite-bearing samples have relatively high concentrations of 25-norhopanes, possibly reflecting a longer history in the subsurface. The samples from recent seepages contain relatively low 25-norhopane contents (Fig. 6), which is expected as the least degraded oils are the least viscous and are able to flow. The samples from Robin's Tump lack 25-norhopanes; these samples are from a well-cemented sequence, and may have been fed from a subsurface migration pathway rather than ingress from the surface. The control samples from two other sequences, where bitumen occurs close to the source rocks, also yielded no norhopanes, which emphasizes that the norhopanes are distinctive to degraded samples.

Several lines of evidence show that at least some bitumen migration occurred in the geological record, rather than recently. The inclusions of quartz in bitumen (Fig. 7a), the cross-cutting relationships between different episodes of bitumen-bearing veins (Fig. 3c), the evidence for forceful migration in bitumen-supported breccias (Fig. 3e) and the evidence for subsequent faulting in slickensided bitumen (Fig. 3f) all imply a geological event. The bitumen was solid in the geological past, showing that it was degraded in the past. The evidence for palaeo-degradation in a fractured reservoir is novel. There are numerous reports of microbial activity in fractured crystalline basement today (cell count data reviewed by McMahon & Parnell 2014). There are also many records of heavy oil or solid bitumen in fractured basement, including occurrences where biodegradation has been demonstrated, such as in the granite of Cornwall (Parnell 1988) and the Western Tatra Mountains basement in Poland (Marynowski *et al.* 2006). However, as in those examples, there is usually no evidence to distinguish between recent biodegradation and palaeo-biodegradation. The observations and data from Shropshire provide the context to demonstrate palaeo-biodegradation.

The framboidal pyrite in the bitumen at Row Brook is a probable consequence of subsurface microbial sulphate reduction (MSR), supported by a light sulphur isotope composition typical of biologically mediated fractionation (Parnell *et al.* 2015). The occurrences of pyrite in the fractured basement are too small for isotopic measurement, but their spatial relationship with bitumen suggests that they may also be the consequence of MSR. Other studies of fractured basement similarly record pyrite with light isotopic compositions interpreted to indicate MSR (Drake *et al.* 2013, 2015; Sahlstedt *et al.* 2013).

Microbial habitat in basement reservoirs

Basement rocks are an important habitat for microbial life, in addition to the overlying sedimentary successions. The colonization of basement fractures in the geological record is documented by a range of evidence, including preserved microfossils (Heim *et al.* 2012), carbon isotope compositions in carbonate precipitates (Sahlstedt *et al.* 2010) and sulphur isotope compositions in pyrite (Drake *et al.* 2013). These occurrences are up to hundreds of metres below the surface. The biomarker data used in this study offer an additional type of evidence for basement-hosted microbial activity.

A fractured basement reservoir may be especially favourable as a subsurface habitat. The basement topographic high (Fig. 1) focuses the up-dip flow of both hydrocarbons and water expelled from the surrounding sedimentary rocks. The basement may be fractured because of the event that uplifted it. Because it is a topographic high on the basement surface, it is more likely to be shallow enough to support microbial life (i.e. at temperatures less than *c.* 80°C; Wilhelms *et al.* 2001), whereas the surrounding sedimentary rocks may be too hot. Nonetheless, the elevated temperatures associated with a subsurface habitat imply that microbial activity was dominated by thermophiles. It is becoming increasingly apparent that thermophiles are involved in the degradation of oil (Cheng *et al.* 2014; Wong *et al.* 2015; Zhou *et al.* in press), partly facilitated by a decrease in oil viscosity and increase in degradation with increasing temperature (Wong *et al.* 2015; Zekri & Chaalal 2005).

Oil reservoirs offer a food source for microbial activity, evidenced by high cell counts in current reservoirs (Takahata *et al.* 2000; Kobayashi *et al.* 2012; Bennett *et al.* 2013). In the geological record, reservoirs will similarly have supported microbial life. Occurrences of sulphides in palaeo-reservoirs (Bata & Parnell 2014; Ellis 2014) may be evidence of this activity. The case study in Shropshire represents a combination of the oil reservoir and fracture habitats.

Conclusions

Combined biomarker and petrographic study of bitumens and their host rocks in fractured sub-Carboniferous basement shows that oil degradation occurred in the geological record. In particular, (1) oil was incorporated in multiple stages of fracturing and mineralization within the basement; (2) the oil was solidified as bitumen in the geological past; (3) the bitumen consistently contains 25-norhopanes, indicating subsurface biodegradation; (4) the most recent (active) seepages contain some 25-norhopanes, indicating that there is a range of compositions with variable degrees of biodegradation. Samples from mineralized fractures show greater degrees of biodegradation.

The observations from the fractured basement in Shropshire add to a growing body of data showing the importance of crystalline basement as a habitat for microbial life, today and in the geological record.

Scientific editing by Graham Shields-Zhou

References

Bata, T. & Parnell, J. 2014. A Neoproterozoic petroleum system in the Dalradian Supergroup, Scottish Caledonides. *Journal of the Geological Society, London*, **171**, 145–148, https://doi.org/10.1144/jgs2013-087

Bennett, B., Fustic, M., Farrimond, P., Huang, H. & Larter, S.R. 2006. 25-norhopanes: formation during biodegradation of petroleum in the subsurface. *Organic Geochemistry*, **37**, 787–797.

Bennett, B., Adams, J.J., Gray, N.D., Sherry, A., Oldenburg, T.B.P. & Huang, H. 2013. The controls on the composition of biodegraded oils in the deep subsurface – part 3. The impact of microorganism distribution on petroleum geochemical gradients in biodegraded petroleum reservoirs. *Organic Geochemistry*, **56**, 94–105.

Bodnar, R.J. 1990. Petroleum migration in the Miocene Monterey Formation, California, USA: constraints from fluid inclusion studies. *Mineralogical Magazine*, **54**, 295–304.

Camden, W. 1722. *Britannia: a Chorographical Description of Great Britain and Ireland, together with the Adjacent Lands*, 2nd edn. Edmund Gibson, London.

Cheng, L., Shi, S., Li, Q., Chen, J., Zhang, H. & Lu, Y. 2014. Progressive degradation of crude oil *n*-alkanes coupled to methane production under mesophilic and thermophilic conditions. *Plos One*, **9**, e113253, https://doi.org/10.1371/journal.pone.0113253

Chopra, S., Lines, L.R., Schmitt, D.R. & Batzle, M.L. 2010. *Heavy Oils: Reservoir Characterization and Production Monitoring*. Society of Exploration Geophysicists, Tulsa, OK.

Compston, W., Wright, A.E. & Toghill, P. 2002. Dating the late Precambrian volcanicity of England and Wales. *Journal of the Geological Society, London*, **159**, 323–339, https://doi.org/10.1144/0016-764901-010

Didyk, B.M., Simoneit, B.R.T. & Eglinton, G. 1983. Bitumen from Coalport Tar Tunnel. *Organic Geochemistry*, **5**, 99–109.

Dines, H.G. 1958. The West Shropshire mining region. *Bulletin of the Geological Survey of Great Britain*, **14**, 1–43.

Drake, H., Åström, M., Tullborg, E.L., Whitehouse, M.J. & Fallick, A.E. 2013. Variability of sulphur isotope ratios in pyrite and dissolved sulphate in granitoid fractures down to 1 km depth – evidence for widespread activity of sulphur reducing bacteria. *Geochimica et Cosmochimica Acta*, **102**, 143–161.

Drake, H., Åström, M.E. *et al.* 2015. Extreme ^{13}C depletion of carbonates formed during oxidation of biogenic methane in fractured granite. *Nature Communications*, **6**, https://doi.org/10.1038/ncomms8020

Ele, M. 1697. An account of the making pitch, tar, and oil out of a blackish stone in Shropshire. *Philosophical Transactions*, **19**, 544.

Ellis, G. 2014. Late authigenic pyrite – An indicator of oil migration and entrapment in the Bonaparte Basin, Timor Sea, Australia. *AAPG International Conference & Exhibition*, September 2014, Istanbul, http://www.searchanddiscovery.com/documents/2014/10655ellis/ndx_ellis.pdf

Greig, D.C., Wright, J.E., Hains, B.A. & Mitchell, G.H. 1968. *Geology of the Country around Church Stretton, Craven Arms, Wenlock Edge and Brown Clee*. Memoir of the Geological Survey of Great Britain.

Grigsby, J.D. 2001. Origin and growth mechanism of authigenic chlorite in sandstones of the Lower Vicksburg Formation, South Texas. *Journal of Sedimentary Research*, **71**, 27–36.

Hamblin, R.J.O. & Coppack, B.C. 1995. *Geology of Telford and the Coalbrookdale Coalfield*. Memoir of the British Geological Survey. Her Majesty's Stationery Office, London.

Heim, C., Lausmaa, J. *et al.* 2012. Ancient microbial activity recorded in fracture fillings from granitic rocks (Äspö Hard Rock Laboratory, Sweden). *Geobiology*, **10**, 280–297.

Kobayashi, H., Kawaguchi, H., Endo, K., Mayumi, D., Sakata, S. & Ikarashi, M. 2012. Analysis of methane production by microorganisms indigenous to a depleted oil reservoir for application in microbial enhanced oil recovery. *Journal of Bioscience and Bioengineering*, **113**, 84–87.

Lamorde, U.A., Parnell, J. & Bowden, S.A. 2015. Constraining the genetic relationships of 25-norhopanes, hopanoic and 25-norhopanoic acids in onshore Niger Delta oils using a temperature-dependent material balance. *Organic Geochemistry*, **79**, 31–43.

Marynowski, L., Gawęda, A., Poprawa, P., Zywiecki, M.M., Kępińska, B. & Merta, H. 2006. Origin of organic matter from tectonic zones in the Western Tatra Mountains Crystalline Basement, Poland: An example of bitumen-source correlation. *Marine and Petroleum Geology*, **23**, 261–279.

McMahon, S. & Parnell, J. 2014. Weighing the deep continental biosphere. *FEMS Microbiology Ecology*, **87**, 113–120.

Morad, S. 1986. SEM study of authigenic rutile, anatase and brookite in Proterozoic sandstones from Sweden. *Sedimentary Geology*, **46**, 77–89.

P'An, C.H. 1982. Petroleum in basement rocks. *AAPG Bulletin*, **66**, 1597–1643.

Parnell, J. 1987. The occurrence of hydrocarbons in Cambrian sandstones of the Welsh Borderland. *Geological Journal*, **22**, 173–190.

Parnell, J. 1988. Migration of biogenic hydrocarbons into granites: a review of hydrocarbons in British plutons. *Marine and Petroleum Geology*, **5**, 385–396.

Parnell, J. 1996. Alteration of crystalline basement rocks by hydrocarbon-bearing fluids: Moinian of Ross-shire, Scotland. *Lithos*, **37**, 281–292.

Parnell, J. 2010. Potential of palaeofluid analysis for understanding oil charge history. *Geofluids*, **10**, 73–82.

Parnell, J. & Monson, B. 1995. Paragenesis of hydrocarbon, metalliferous and other fluids in Newark Group basins, eastern U.S.A. *Transactions of the Institution of Mining and Metallurgy (Earth Sciences)*, **104**, 136–144.

Parnell, J., Robinson, N. & Brassell, S. 1991. Discrimination of bitumen sources in Precambrian and Lower Palaeozoic rocks, southern U.K., by gas chromatography–mass spectrometry. *Chemical Geology*, **90**, 1–14.

Parnell, J., Carey, P. & Monson, B. 1998. Timing and temperature of decollement on hydrocarbon source rock beds in cyclic lacustrine successions. *Palaeogeography, Palaeoclimatology, Palaeoecology*, **140**, 121–134.

Parnell, J., Middleton, D., Chen, H. & Hall, D. 2001. The use of integrated fluid inclusion studies in constraining oil charge history and reservoir compartmentation: examples from the Jeanne d'Arc Basin, offshore Newfoundland. *Marine and Petroleum Geology*, **18**, 535–549.

Parnell, J., Bellis, D., Feldmann, J. & Bata, T. 2015. Selenium and tellurium in palaeo-oil reservoirs. *Journal of Geochemical Exploration*, **148**, 169–173.

Pattrick, R.A.D. & Bowell, R.J. 1991. The genesis of the West Shropshire Orefield: evidence from fluid inclusions, sphalerite chemistry, and sulphur isotopic ratios. *Geological Journal*, **26**, 101–115.

Pauley, J.C. 1990. Sedimentology, structural evolution and tectonic setting of the late Precambrian Longmyndian Supergroup of the Welsh Borderland, UK. *In*: D'Lemos, R.S., Strachan, R.A. & Topley, C.G. (eds) *The Cadomian Orogeny*. Geological Society, London, Special Publications, **51**, 341–351, https://doi.org/10.1144/GSL.SP.1990.051.01.22

Peters, K.E. & Moldowan, J.M. 1993. *The Biomarker Guide: Interpreting Molecular Fossils in Petroleum and Ancient Sediments*. Prentice Hall, Englewood Cliffs, NJ.

Peters, K.E., Moldowan, J.M., McCaffrey, M.A. & Fago, F.J. 1996. Selective biodegradation of extended hopanes to 25-norhopanes in petroleum reservoirs. Insights from molecular mechanics. *Organic Geochemistry*, **24**, 765–783.

Petford, N. & McCaffrey, K. (eds) 2003. *Hydrocarbons in Crystalline Rocks*. Geological Society, London, Special Publications, **214**, https://doi.org/10.1144/GSL.SP.2003.214.01.01

Plant, J.A., Jones, D.G. & Haslam, H.W. 1999. *The Cheshire Basin: Basin Evolution, Fluid Movement and Mineral Resources in a Permo-Triassic Rift Setting*. British Geological Survey, Keyworth.

Plot, R. 1684. A discourse concerning the sepulchral lamps of the ancients, shewing the possibility of their being made divers waies. *Philosophical Transactions*, **14**, 806–811.

Pocock, R.W., Whitehead, T.H., Wedd, C.B. & Robertson, T. 1938. *Shrewsbury District*. Memoir of the Geological Survey of Great Britain. His Majesty's Stationery Office, London.

Sahlstedt, E., Karhu, J.A. & Pitkänen, P. 2010. Indications for the past redox environments in deep groundwaters from the isotopic composition of carbon and oxygen in fracture calcite, Olkiluoto, SW Finland. *Isotopes in Environmental and Health Studies*, **46**, 370–391.

Sahlstedt, E., Karhu, J.A., Pitkänen, P. & Whitehouse, M. 2013. Implications of sulfur isotope fractionation in fracture-filling sulphides in crystalline bedrock, Olkiluoto, Finland. *Applied Geochemistry*, **32**, 52–69.

Schutter, S.R. 2003. Occurrences of hydrocarbons in and around igneous rocks. *In*: Petford, N. & McCaffrey, K.J.W. (eds) *Hydrocarbons in Crystalline Rocks*. Geological Society, London, Special Publications, **214**, 83–92, https://doi.org/10.1144/GSL.SP.2003.214.01.03

Seifert, W.K. & Moldowan, J.M. 1979. The effect of biodegradation on steranes and terpanes in crude oils. *Geochimica et Cosmochimica Acta*, **43**, 111–126.

Takahata, Y., Nishijima, M., Hoaki, T. & Maruyama, T. 2000. Distribution and physiological characteristics of hyperthermophiles in the Kubiki oil reservoir in Niigata, Japan. *Applied and Environmental Microbiology*, **66**, 73–79.

Tong, K., Zhao, C. *et al.* 2012. Reservoir evaluation and fracture characterization of the metamorphic buried hill reservoir in Bohai Bay Basin. *Petroleum Exploration and Development*, **39**, 62–69.

Trice, R. 2014. Basement exploration, West of Shetlands: progress in opening a new play on the UKCS. *In*: Cannon, S.J.C. & Ellis, D. (eds) *Hydrocarbon Exploration to Exploitation West of Shetlands*. Geological Society, London, Special Publications, **397**, 81–105, https://doi.org/10.1144/SP397.3

Van Panhuys-Sigler, M. & Trewin, N.H. 1990. Authigenic sphene cement in Permian sandstones from Arran. *Scottish Journal of Geology*, **26**, 139–144, https://doi.org/10.1144/sjg26020139

Wang, G., Wang, T.G., Simoneit, B.R.T. & Zhang, L. 2013. Investigation of hydrocarbon biodegradation from a downhole profile in Bohai Bay Basin: Implications for the origin of 25-norhopanes. *Organic Geochemistry*, **55**, 72–84.

Wang, G., Wang, T.G., Han, K., Wang, L. & Chi, S. 2015. Recognition of a novel Precambrian petroleum system based on isotopic and biomarker evidence in the Yangtze platform, South China. *Marine and Petroleum Geology*, **68**, 414–426.

Wilhelms, A., Larter, S.R., Head, I., Farrimond, P., di-Primio, R. & Zwach, C. 2001. Biodegradation of oil in uplifted basins prevented by deep-burial sterilization. *Nature*, **411**, 1034–1037.

Wong, M.-L., An, D. *et al.* 2015. Roles of thermophiles and fungi in bitumen degradation in mostly cold oil sands outcrops. *Applied and Environmental Microbiology*, **81**, 6825–6838.

Woodcock, N.H. 1984. The Pontesford Lineament, Welsh Borderland. *Journal of the Geological Society*, **141**, 1001–1014, https://doi.org/10.1144/gsjgs.141.6.1001

Zekri, A.Y. & Chaalal, O. 2005. Effect of temperature on biodegradation of crude oil. *Energy Sources*, **27**, 233–244.

Zhou, J.F., Gao, P.K. *et al.* In press. Heavy hydrocarbon degradation of crude oil by a novel thermophilic *Geobacillus stearothermophilus* strain A-2. *International Biodeterioration & Biodegradation*. corrected proof online October 8, 2016, https://doi.org/10.1016/j.ibiod.2016.09.031